ORGANOMETALLICS

Volume 24, Number 10, May 9, 2005

Communications

Mechanism of Endo−Exo Interconversion in η^3-Allyl Cp Complexes: A Longstanding Unresolved Issue

Alireza Ariafard, Siwei Bi, and Zhenyang Lin*

Department of Chemistry, The Hong Kong University of Science and Technology, Clear Water Bay, Kowloon, Hong Kong

Received March 6, 2005

Summary: Density functional theory studies of the d^6 allyl complexes $CpM(CO)(\eta^3\text{-}C_3H_5)$ (M = Fe, Ru) and the d^4 allyl complex $CpMo(CO)_2(\eta^3\text{-}C_3H_5)$ show that the interconversion for $CpMo(CO)_2(\eta^3\text{-}C_3H_5)$ through the $\eta^3 \rightarrow \eta^3 \rightarrow \eta^3$ pathway is intrinsically more favorable than the $\eta^3 \rightarrow \eta^1 \rightarrow \eta^3$ pathway. However, the η^3 transition states for $CpM(CO)(\eta^3\text{-}C_3H_5)$ (M = Fe, Ru) are inaccessible, because one pair of the six metal d electrons has to occupy a d orbital having significant metal−Cp antibonding character in the transition structure.

Transition-metal η^3-allyl complexes are important intermediates in many catalytic reactions.[1] These complexes have attracted considerable interest both experimentally[2] and theoretically.[3] It is well-known that these complexes can exist as endo and exo isomers. The relative endo−exo stability has been systematically investigated recently.[4] While the factors determining the relative stability are now well understood, there is still an important question regarding the mechanism of the endo−exo interconversion[5] that remains to be answered. In the 1960s, it was already established that the endo−exo interconversion in $CpMo(CO)_2(\eta^3\text{-allyl})$ proceeds by a mechanism equivalent to rotation of the planar π-allyl moiety about a molybdenum−allyl axis: i.e., an $\eta^3 \rightarrow \eta^3 \rightarrow \eta^3$ pathway.[6] Interestingly, for d^6-$CpM(CO)(\eta^3\text{-allyl})$, where M is iron[7] or ruthenium,[8] the endo−exo interconversion was found to proceed by an $\eta^3 \rightarrow \eta^1 \rightarrow \eta^3$ pathway in which an η^1 intermediate species is involved. Although the interconversion mechanisms were clearly established from NMR experiments as early as the 1960s, the reasons the molybdenum Cp complexes differ mechanistically from the Cp complexes of the iron group in the endo−exo interconversion are

* To whom correspondence should be addressed. E-mail: chzlin@ust.hk.

(1) See for example: (a) Fernandes, R. A.; Stimac, A.; Yamamoto, Y. *J. Am. Chem. Soc.* **2003**, *125*, 14133. (b) Ng, S. H. K.; Adams, C. S.; Hayton, T. W.; Legzdins, P.; Patrick, B. O. *J. Am. Chem. Soc.* **2003**, *125*, 15210. (c) Brunkan, N. M.; Brestensky, D. M.; Jones, W. D. *J. Am. Chem. Soc.* **2004**, *126*, 3627. (d) Trost, B. M.; van Vranken, D. L. *Chem. Rev.* **1996**, *96*, 395. (e) Helmchen, G.; Pfalz, A. *Acc. Chem. Res.* **2000**, *33*, 336.

(2) See for example: (a) Kondo, H.; Yamaguchi, Y.; Nagashima, H. *Chem. Commun*. **2000**, 1075. (b) Liu, G.; Beetstra, D. J.; Meetsma, A.; Hessen, B. *Organometallics* **2004**, *23*, 3914. (c) Borgmann, C.; Limberg, C.; Kaifer, E.; Pritzkow, H.; Zsolnai, L. *J. Organomet. Chem.* **1999**, *580*, 214. (d) Matsushima, Y.; Onitsuka, K.; Takahashi, S. *Organometallics* **2004**, *23*, 3763. (e) Yih, K. H.; Lee, G. H.; Huang, S. L.; Wang, Y. *Organometallics* **2002**, *21*, 5767. (f) Wakefield, J. B.; Stryker, J. M. *Organometallics* **1990**, *9*, 2428.

(3) See for example: (a) Cedeño, L. D.; Weitz, E. *Organometallics* **2003**, *22*, 2652. (b) Swang, O.; Blom, R. *J. Organomet. Chem.* **1998**, *561*, 29. (c) Tobisch, S.; Taube, R. *Organometallics* **1999**, *18*, 3045. (d) Suzuki, T.; Okada, G.; Hioki, Y.; Fujimoto, H. *Organometallics* **2003**, *22*, 3649. (e) Clot, E.; Eisenstein, O.; Weng, T. S.; Penner-Hahn, J.; Caulton, K. G. *J. Am. Chem. Soc.* **2004**, *126*, 9079. (f) Solin, N.; Szabó, I. *Organometallics* **2001**, *20*, 5464.

(4) (a) Bi, S.; Ariafard, A.; Jia, G.; Lin, Z. *Organometallics* **2005**, *24*, 680. (b) Xue, P.; Bi, S.; Sung, H. H. Y.; Williams, I. D.; Lin, Z.; Jia, G. *Organometallics* **2004**, *23*, 4735.

(5) Crabtree, R. H. *The Organometallic Chemistry of the Transition Metals*; Wiley: New York, 2001; p 122.

(6) (a) Rode, W. C.; Davison, A. *Inorg. Chem*. **1967**, *6*, 2124. (b) Faller, J. W.; Incorvia, M. J. *Inorg. Chem.* **1968**, *7*, 840.

(7) Fish, R. W.; Giering, W. P.; Marten, D.; Rosenblum, M. *J. Organomet. Chem.* **1976**, *105*, 101.

(8) Gibson, D. H.; Hsu, W.-L.; Steinmetz, A. L.; Johnson, B. V. *J. Organomet. Chem.* **1981**, *208*, 89.

10.1021/om050161h CCC: $30.25
Publication on Web 04/05/2005

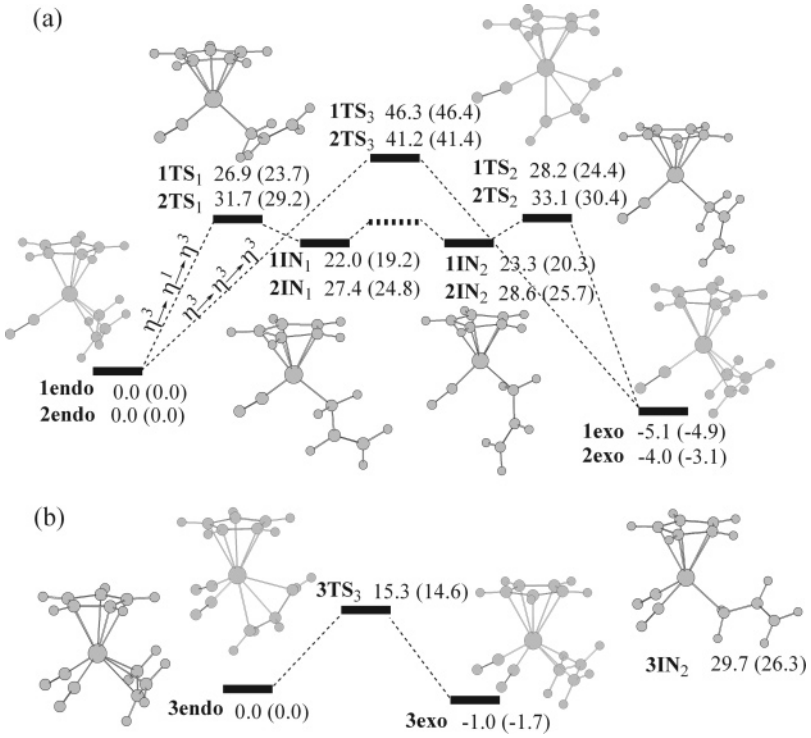

Figure 1. Energy profiles for the exo−endo interconversion in (a) **1** and **2** and (b) **3**. The relative energies and free energies (in parentheses) are given in kcal/mol.

still unclear. The question has long intrigued researchers who have worked in the area. In the literature, there have been many theoretical and experimental discussions on the endo−exo interconversion.[9] However, up to now, no explanations have been found. In this communication, we wish to provide better insight into the question through density functional theory calculations[10] on the model complexes CpM(CO)(η^3-C_3H_5) (M = Fe, Ru; **1** and **2**) and CpMo(CO)$_2$(η^3-C_3H_5) (**3**).

Figure 1 shows the results of calculations on the model complexes. Consistent with the experimental finding that **1** and **2** favor a mechanism in which an η^1 intermediate is involved, the $\eta^3 \rightarrow \eta^1 \rightarrow \eta^3$ pathway was found to have much lower reaction barriers than the $\eta^3 \rightarrow \eta^3 \rightarrow \eta^3$ pathway (Figure 1a). For **3**, the calculations clearly show that the barrier for a direct 180° rotation of the allyl group about the metal−allyl axis is surprisingly low (Figure 1b). The barriers of the $\eta^3 \rightarrow \eta^1 \rightarrow \eta^3$ pathways for all the complexes calculated are comparable, indicating that the barriers are closely related to the metal−ligand bond dissociation energies. The free energy barriers of the endo → exo transformation through the favorable $\eta^3 \rightarrow \eta^1 \rightarrow \eta^3$ pathway for **1** and **2** were calculated to be 24.4 and 30.4 kcal/mol**,** respectively. The higher barrier for **2** reflects a greater Ru−ligand interaction as compared to the Fe−ligand interaction. For **3**, the barrier of the endo → exo transformation through a simple 180° rotation of the allyl ligand was found to be 14.6 kcal/mol. These results converge nicely to the experimental values of 24.1 kcal/mol for CpFe(CO)(η^3-C_3H_5),[7] 28.9 kcal/mol for CpRu(CO)(η^3-C_3H_5),[8] and 15.5 kcal/mol for CpMo(CO)$_2$(η^3-C_3H_5).[9c,d] The agreement clearly suggests the high accuracy of our calculations. For **3**, we were unable to locate the transition state connecting **3exo** and **3IN$_2$**, probably due to the flatness in the potential energy surface from the transition state to the intermediate **3IN$_2$**.

The most important issue now is to understand why the $\eta^3 \rightarrow \eta^3 \rightarrow \eta^3$ pathway in **1** or **2** is less favorable as compared to the $\eta^3 \rightarrow \eta^1 \rightarrow \eta^3$ pathway but the former pathway is more favorable in **3**. Comparison of the frontier molecular orbitals for the species involved provides insight into this important issue. Figure 2 shows the orbital correlation diagram of the five metal d orbitals for **2exo** and **2TS$_3$**. For **2exo**, the three orbitals that accommodate the six metal d electrons correspond to the three highest occupied molecular orbitals (HOMOs). The HOMO and HOMO-2, which are the d_{xy} and d_{z^2} orbitals, are stabilized through metal→π^* (carbonyl) back-donation interaction. However, the d_{xy} orbital is higher in energy than the d_{z^2} orbital, due to its antibonding interaction with the occupied π_2 orbital of the η^3-allyl anionic ligand. An allyl ligand has three molecular orbitals: i.e., bonding (π_1), nonbonding (π_2) and antibonding (π_3).[5] The HOMO-1 is $d_{x^2-y^2}$ and has a slightly bonding interaction with the unoccupied π_3 orbital of the η^3-allyl anionic ligand. The two lowest unoccupied molecular orbitals, LUMO and LUMO+1, correspond to d_{yz} and d_{xz}, respectively. These two unoccupied metal d orbitals have antibonding interactions with both the Cp and allyl ligands' π orbitals.

For the transition state **2TS$_3$**, the three occupied orbitals are d_{xz}, $d_{x^2-y^2}$ and d_{xy}. The two unoccupied

(9) (a) Schilling, B. E. R.; Hoffmann, R.; Faller, J. W. *J. Am. Chem. Soc.* **1979**, *101*, 592. (b) Webster, C. E.; Hall, M. B. *Organometallics* **2001**, *20*, 5606. (c) van Staveren, D. D.; Weyhermüller, T.; Metzler-Nolte, N. *Organometallics* **2000**, *19*, 3730. (d) Faller, J. W.; Chen, C.-C.; Mattina, M. J.; Jakubowski, A. *J. Organomet. Chem.* **1973**, *52*, 361. (e) Cosford, D. P. N.; Liebeskind, L. S. *Organometallics* **1994**, *13*, 1498. (f) Ascenso, J. R.; Dias, R. A.; Fernandes, J. A.; Martins A. M.; Rodrigues S. S. *Inorg. Chim. Acta* **2003**, *356*, 279. (g) Curtis, M. D.; Eisenstein, O. *Organometallics* **1984**, *3*, 887.

(10) See the Supporting Information for details.

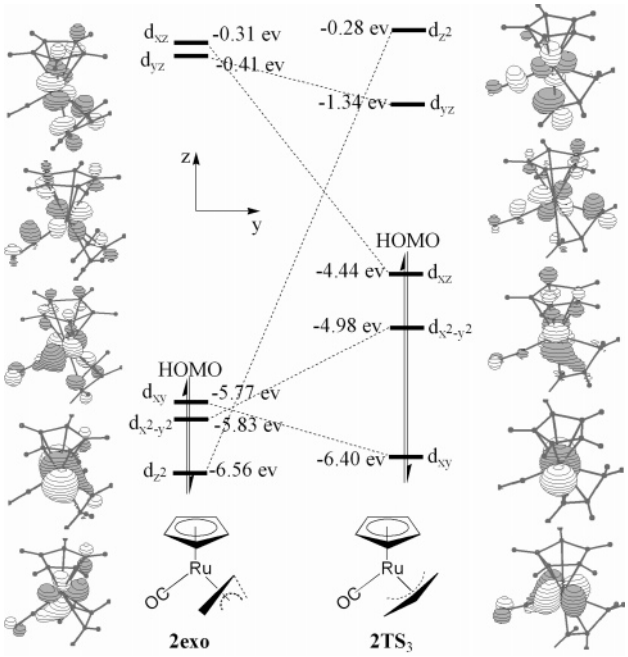

Figure 2. Orbital correlation diagram for the d orbitals of **2exo** and **2TS$_3$**. The d orbitals labeled are approximate, for the purpose of discussion.

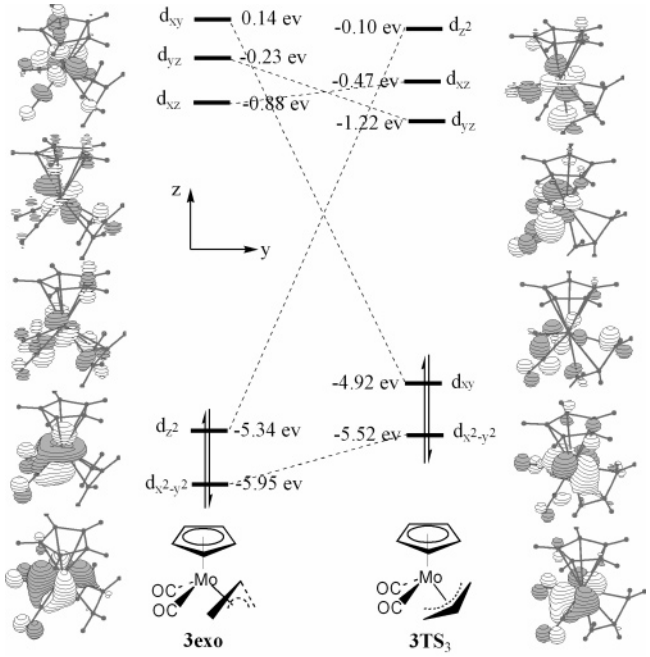

Figure 3. Orbital correlation diagram for the d orbitals of **3exo** and **3TS$_3$**.

orbitals become d_{yz} and d_{z^2}. Compared to those in **2exo**, both the d_{xy} and d_{yz} orbitals in **2TS$_3$** are slightly stabilized, while the $d_{x^2-y^2}$ orbital is destabilized. The rotation of the η^3-allyl ligand from **2exo** to **2TS$_3$** reduces the antibonding interaction between d_{xy} and the π_2 orbital of the η^3-allyl ligand. Simultaneously, the rotation also reduces the bonding interaction between $d_{x^2-y^2}$ and the π_3 orbital of the η^3-allyl ligand. The correlation diagram shows that drastic changes occur for the d_{z^2} and d_{xz} orbitals. In **2exo**, the d_{z^2} orbital is the lowest among the five d orbitals. In **2TS$_3$**, it is the highest, however, because it is strongly antibonding with one terminal carbon p_π of the η^3-allyl ligand. In **2exo**, the d_{xz} orbital is unoccupied. In **2TS$_3$**, it becomes occupied and is the HOMO. For the d_{xz} (HOMO) orbital in the transition state, the orientation of the η^3-allyl ligand minimizes its antibonding interaction with the orbitals from the η^3-allyl ligand. However, its antibonding interaction with the Cp's orbital remains. Therefore, a crucial cause of the remarkable instability of the transition state **2TS$_3$** (or **1TS$_3$**) can be attributed to occupation of the d_{xz} (HOMO) orbital, which significantly weakens the metal−Cp bonding interactions. Calculations show that the average metal−C(Cp) distances in **1TS$_3$** and **2TS$_3$** are about 0.010−0.050 Å longer than those in their stable endo and exo structures.[10] **1TS$_3$** is relatively higher than **2TS$_3$**, likely because of its more crowded ligand arrangement due to the smaller size of the Fe center in comparison with Ru.

Figure 3 shows the correlation diagram of the d orbitals of **3**. **3** can be formally described as a d^4 complex. The HOMO and HOMO-1 correspond to d_{z^2} and $d_{x^2-y^2}$. The three unoccupied d orbitals are d_{xz}, d_{yz}, and d_{xy}. The 90° rotation of the allyl ligand in **3**, similar to **1** and **2**, destabilizes the d_{z^2} orbital and causes it to be the LUMO+2. Opposite to what was seen for **1** and **2**, the rotation does not stabilize the d_{xz} orbital. Instead, the rotation causes the d_{xy} orbital to be the HOMO, because

Scheme 1

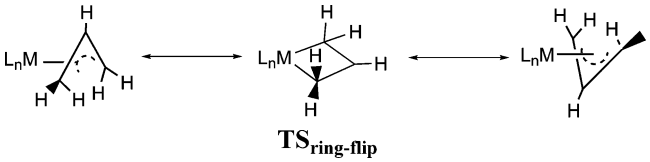

the rotation turns off the strong σ^*-antibonding interactions. The d_{xz} and d_{yz} orbitals, having the metal−Cp antibonding character, again remain the lowest unoccupied molecular orbitals (LUMO+1 and LUMO). Unlike in the d^6 systems, the situation in the d^4 system is that the two d orbitals, which accommodate the four d electrons in the η^3 transition state **3TS$_3$**, do not have significant metal−ligand antibonding character. Therefore, the η^3 transition state **3TS$_3$** is relatively much more stable than the corresponding transition states in the d^6 systems (**1TS$_3$** and **2TS$_3$**). This is further supported by comparison of the energy difference between the HOMOs of the exo isomer and its η^3 transition state (1.52 eV for **1**, 1.33 eV for **2** and 0.042 eV for **3**).

There is also one other possible pathway for the endo−exo interconversion involving a bis-η^1 transition state, shown in Scheme 1. This pathway is similar to the "ring-flip" process of the metallacyclic five-membered ring in many group 4 metal−(*s*-*cis*-butadiene) complexes.[11] The ring-flip transition states (**TS$_{ring-flip}$**) lie very high on the potential energy surface (49.1, 55.4, and 58.5 kcal/mol in the free energy for **1TS$_{ring-flip}$**, **2TS$_{ring-flip}$**, and **3TS$_{ring-flip}$** relative to their stable endo structures, respectively). These results are consistent with the findings reported by Webster and Hall for $[CpIr(PH_3)(allyl)]^+$.[9b] In the ring-flip transition structures, all the carbon atoms of the allyl ligand and the metal center lie approximately on a common plane. This

(11) (a) Yasuda, H.; Kajihara, Y.; Mashima, K.; Nagasuna, K.; Lee, K.; Nakamura, A. *Organometallics* **1982**, *1*, 388. (b) Prins, T. J.; Hauger, B. E.; Vance, P. J.; Wemple, M. E.; Kort, D. A.; O'Brien, J. P.; Silver, M. E. *Organometallics* **1991**, *10*, 979.

structural arrangement turns off the back-bonding interaction between the metal center and the middle carbon of the allyl ligand and, at the same time, produces a large ring strain because of the approximately planar four-membered-ring structure. To estimate the contribution of the ring strain to the instability of the transition states $\mathbf{TS_{ring-flip}}$, we also calculated the barrier height of the ring-flip process for the d^0 allyl complex $[Zr(Cp)_2(allyl)]^+$, in which there is no metal(d)-to-allyl(π^*) back-bonding interaction. The large barrier of 43.1 kcal/mol implies that the ring strain plays a crucial role. In the d^0 complex, we found that the $\eta^3 \rightarrow \eta^1 \rightarrow \eta^3$ pathway, having an approximate barrier of 21.7 kcal/mol, is responsible for the interconversion. The three frontier orbitals available for ligands in a bent $[Cp_2Zr]^{2+}$ fragment have their maximum amplitudes in the plane perpendicular to the Ct−Zr−Ct plane (Ct is the centriod of the Cp ring). It is therefore understandable that the $\eta^3 \rightarrow \eta^3 \rightarrow \eta^3$ pathway is not possible, because the relevant transition state has a structure in which the allyl ligand cannot be stabilized by the available frontier orbitals of the metal fragment.

In summary, the significant difference between $\mathbf{1TS_3}$ (or $\mathbf{2TS_3}$), the η^3 transition state for the d^6 system $CpML(\eta^3\text{-allyl})$, and $\mathbf{3TS_3}$, the η^3 transition state for the d^4 system $CpML_2(\eta^3\text{-allyl})$, can be described as follows. In $\mathbf{1TS_3}$ (or $\mathbf{2TS_3}$), one pair of the six metal d electrons has to occupy a d orbital having significant metal−Cp antibonding character because of the ligand arrangement in the transition state. In the η^3 transition state for the d^4 system $CpML_2(\eta^3\text{-allyl})$, the metal d electrons occupy two d orbitals which do not contain significant metal−ligand antibonding character. Therefore, for the d^4 system $CpML_2(\eta^3\text{-allyl})$ the $\eta^3 \rightarrow \eta^3 \rightarrow \eta^3$ pathway is expected to be intrinsically more favorable than the $\eta^3 \rightarrow \eta^1 \rightarrow \eta^3$ pathway. This conclusion is supported by the fact that many other d^4 complexes were found to have the endo−exo interconversion via the $\eta^3 \rightarrow \eta^3 \rightarrow \eta^3$ pathway.[9c−f] For a d^6 system $CpM(\eta^3\text{-allyl})(L)$, the $\eta^3 \rightarrow \eta^1 \rightarrow \eta^3$ pathway is generally more favorable. Here, we anticipate that when a Cp ring slippage, which can alleviate the metal−Cp antibonding in the HOMO of the η^3 transition state, is possible, the $\eta^3 \rightarrow \eta^3 \rightarrow \eta^3$ pathway for the d^6 system $CpML(\eta^3\text{-allyl})$ could become competitive. Webster and Hall reported that the η^3 transition state for the endo−exo interconversion in $[CpIr(\eta^3\text{-allyl})(PH_3)]^+$ has a significant ring slippage.[9b] The barrier of the $\eta^3 \rightarrow \eta^3 \rightarrow \eta^3$ pathway is higher than that of the $\eta^3 \rightarrow \eta^1 \rightarrow \eta^3$ pathway by about 3.7 kcal/mol only. In contrast, the barrier differences between the $\eta^3 \rightarrow \eta^3 \rightarrow \eta^3$ and $\eta^3 \rightarrow \eta^1 \rightarrow \eta^3$ pathways are substantially large, 18.1 kcal/mol for **1** and 8.1 kcal/mol for **2**, because the η^3 transition states do not have a similar ring slippage.

Acknowledgment is made to the Hong Kong Research Grants Council (Grant No. HKUST 6023/04P).

Supporting Information Available: Tables giving Cartesian coordinates and computational details. This material is available free of charge via the Internet at http://pubs.acs.org.

OM050161H